INDENTATION OF THIN COATINGS: THEORETICAL AND EXPERIMENTAL INVESTIGATION

SERGEI M. AIZIKOVICH[1], ANDREY L. NIKOLAEV[1], EVGENIY V. SADYRIN[1], LEONID I. KRENEV[1], VLADIMIR A. IRKHA[2] & ALEXANDER N. GALYBIN[3]
[1]Don State Technical University, Russia
[2]K.G. Razumovsky Moscow State University of Technologies and Management, Russia
[3]The Schmidt Institute of Physics of the Earth (IPE RAS), Russia

ABSTRACT

An effective mathematical model is proposed for describing the experiment on indentation of samples with layered or functionally graded coatings. It is based on the solution of the contact problem of the theory of elasticity of indentation of a punch into elastic half-space with a coating. The results of mathematical modelling and experiments on indentation of the ZnO coating manufactured by the method of pulsed laser deposition on a silicon substrate are compared. The microgeometrical characteristics, as well as the chemical composition of the coating, were studied.

Keywords: nanoindentation, layered composite, coating, scanning electron microscopy, atomic force microscopy, mathematical modelling.

1 INTRODUCTION

The idea of continuous recording of the “stress–strain” curve originated in the middle of the 20th century [1], and was developed in the 1970s of the 20th century [2], [3]. However, a number of technical difficulties did not allow the use of such methods to extract the physical characteristics of the material from primary data. In the 1980s, with the development of the instrumental base at the leading universities for measuring the mechanical characteristics of materials, nanoindentation became more and more widespread as a group of methods using precise local force action on the material and simultaneous recording of deformation responses with the resolution of order of nanometer [4], [5].

A new impetus to the development of nanoindentation was given by the classic work by Oliver and Pharr [6], who proposed a method for analysing the results of indentation using one of the most popular indenter tip shapes, a pyramidal one with a triangular cross section and a rounded tip (Berkovich indenter). The result of the experiment is the dependence of the indenter penetration depth on the applied load (the force–displacement curve). Since it is difficult to avoid plastic deformation during the experiment, it has been proposed (in contrast to the linear approximation previously used by Doerner and Nix [7]) to analyse the unloading part of the force-displacement curve in order to determine the elastic properties of the sample. They described a technique for determining the Young’s modulus of a sample based on the analysis of indentation stiffness, i.e. the rate of the load change with respect to the indenter penetration depth at the maximum indentation depth. In this case, it is necessary to know the area of the contact zone. For homogeneous materials, it is determined by calibration by using the samples with previously studied properties.

The Oliver–Pharr method works for a wide range of materials, and the reconstructed value of Young’s modulus is close to the real value of Young’s modulus of the material, determined by traditional test methods [8]. This method is also used to study the mechanical properties of biological tissues [9]–[12]. In addition, in some cases, the use of this method provides predictable results when indenting material layers, when the penetration depth does not exceed 10% of its thickness [13]–[15]. However, with a significant difference in Young’s moduli of the layers, the reconstructed value of Young’s modulus can be noticeably

WIT Transactions on Engineering Sciences, Vol 134, © 2022 WIT Press
www.witpress.com, ISSN 1743-3533 (on-line)
doi:10.2495/BE450141

underestimated or overestimated. It was shown that the presence of an inhomogeneous or layered coating in a material significantly affects the size of the contact zone [16]–[18]. In addition, this approach cannot be applied to determine Young's moduli of thin coatings or layers of material, since the required penetration depth becomes comparable to the surface roughness height. All this requires the development of indentation models that take into account the inhomogeneity in depth of the sample under study, and on their basis, methods for interpreting the experimental results obtained.

Direct numerical methods, such as the finite element method (FEM) are predominantly used in the literature for the analysis of nanoindentation. Kot et al. [19] proposed a technique for studying the mechanical characteristics of coating-substrate systems based on a combination of the results of spherical indentation and FEM. Karimpour et al. [20] proposed a method for determining Young's modulus, hardness, and yield strength for single- and multilayer structures using the FEM and nanoindentation experiment. Dean et al. [21] measured the indentation hardness and the residual stresses in two-layer samples using the FEM. Veprek-Heijman and Veprek [22] used FEM to study nonlinear deformation of soft substrates when an indenter penetrates into hard or super-hard coatings.

In this work, in order to describe the process of nanoindentation, an effective mathematical model is proposed that takes into account the layered or continuously inhomogeneous structure of the sample. ZnO coatings are considered, which are used in practice, e.g. in photocatalytic filters [23], [24], solar cells [25]–[27], gas sensors [28]–[30], medical devices [31], and other applications of modern electronics (including nanorods [32]–[36]).

2 EXPERIMENTAL SETUP

2.1 Materials and preparation of samples

A ZnO-coated sample on Si (001) substrate was obtained by pulsed laser deposition. The deposition parameters were as follows: power density of laser radiation 2 J/cm^2, target-substrate distance 5 cm, synthesis temperature 500°C, oxygen pressure during deposition 2*10^{-2} mbar, laser pulse energy 200 mJ, pulse repetition rate 10 Hz. The target was made of pure ZnO (ceramic), 6000 laser pulses were performed to deposit the coating.

The substrate was pre-cleaned in four steps:

1. Boiling in acetone;
2. Boiling in a mixture of acetic acid and hydrogen peroxide (1:1 by volume);
3. Etching in 2% HCl solution;
4. Washing in deionised water.

2.2 Microgeometrical properties of the coating

The coating thickness was measured by a Crossbeam 340 scanning electron microscope, SEM, (Carl Zeiss Microscopy Gmbh, Germany) using an Everhart–Thornley detector at the accelerating voltage of 1.5 kV. To do this, a cross section was made in the coating using a focused ion beam (Fig. 1). The measured coating thickness was 647.6 nm.

Further on, the surface roughness of the sample was measured using an atomic force microscope (AFM) Nanoeducator (NT-MDT, Russia). The study of the microgeometrical characteristics of the surface of both substrate and coating was carried out using the same AFM equipped with a tungsten probe. Before conducting the measurements, the probe has been calibrated on a test grid.

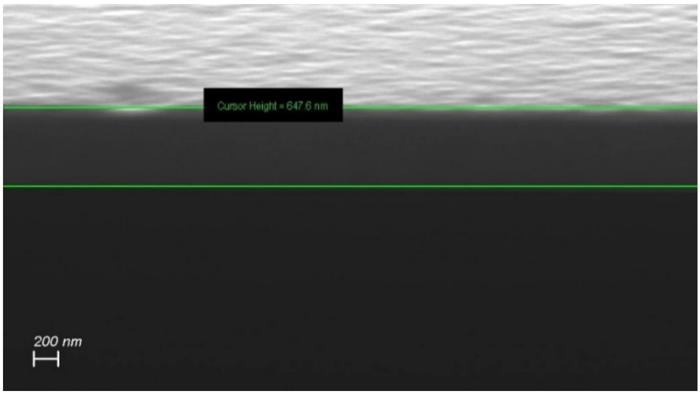

Figure 1: Measurement of ZnO coating thickness on SEM.

The average roughness R_a and the maximum roughness height R_t have been calculated using the Gwyddion software (Czech Metrology Institute, Czech Republic). Twelve profiles were obtained for each image in 3D (horizontal, vertical, diagonal) and the averaged R_a values have been calculated. Each profile represent an average over five neighbouring profiles parallel to it. The measurement areas were 15 × 15 µm for substrate and 45 × 45 µm for coating. The results of measurements are summarised in Table 1.

Table 1: Microgeometrical characteristics of the coating and substrate.

Sample	Average Ra over 15 profiles (nm)	Standard deviation (nm)	Rt (nm)
Substrate Si	12.09	1.57	181.6
Coating ZnO	11.30	1.43	154.6

The results of measurements show that the coating surface has a slight roughness and a poorly developed topography. Some defects of deposition in the form of small caverns are visible on the SEM image (Fig. 1), however, none of them fell into the AFM scanning field (Fig. 2(a)).

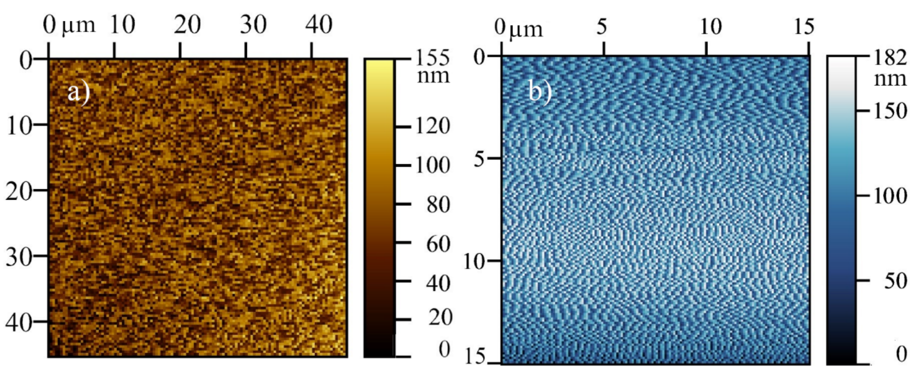

Figure 2: Surface topology. (a) ZnO coatings; and (b) Substrate.

2.3 The chemical composition of the coating

Using X-ray energy-dispersive spectroscopy (EDX, Oxford Instruments, UK), the elemental composition of the coating was studied. The analysis has been conducted in six areas of the sample. Table 2 shows the averaged values for all the studied areas of the coating surface. It follows from this study that the samples consist only of oxygen and zinc atoms and do not have any impurities.

Table 2: Average elemental composition of the coating.

Area	1	2	3	4	5	6
O %	41.31	41.17	41.29	45.10	45.07	44.93
Zn %	58.69	58.83	58.71	54.90	54.93	55.07
Sum %	100.00	100.00	100.00	100.00	100.00	100.00

3 NANOINDENTATION

In order to estimate the mechanical properties of the coating, a series of nanoindentation experiments were carried out on the Nanotest 600 Platform 3 test machine (Micro Materials, UK) using a Berkovich diamond indenter. The experiments were carried out at a constant temperature of 27.0 ± 0.1°C in a closed chamber. Before the experiments, instrument calibrations were performed using reference samples of fused quartz and sapphire.

Since the sample is a "Si (001) substrate – ZnO coating" system, the properties of the substrate were studied firstly (after the sample preparation). A series of 8 indentations were made at a distance of at least 5 indent diameters from each other with an increasing force in the range 1 mN $\leq P_{max} \leq$ 100 mN, while the maximum indentation depth varied in the range 33 nm $\leq h_{max} \leq$ 662 nm. The analysis of the force-displacement curves was performed in accordance with the Oliver–Pharr method. The value of Poisson's ratio of the substrate was assumed to be ν = 0.27 [37]. Thus, reduced Young's modulus E_r, Young's modulus E, and indentation hardness H were found as follows 158.97 ± 5.86 GPa, 171.64 ± 7.31 GPa, and 10.62 ± 1.08 GPa, respectively.

To evaluate the properties of the ZnO coating, a series of 12 indentations were made at a distance of at least five indent diameters from each other with an increasing force in the range 1 mN$\leq P_{max} \leq$ 200 mN for the maximum indentation depth of 30 nm$\leq h_{max} \leq$ 955 nm. Typical curves for maximum indentation forces of 4, 20, 70, and 200 mN are shown in Fig. 3. Poisson's ratio of ZnO was assumed to be ν = 0.25 [38].

3.1 Mathematical modelling of experiments

For the mathematical description of the indentation process an effective mathematical model was proposed. In its framework a non-deformable conical punch is pressed into the surface Γ of an elastic half-space Ω consisting of an inhomogeneous layer (coating) of thickness H and a homogeneous half-space (substrate). A cylindrical coordinate system ρ, φ, z is associated with the half-space; the z-axis is normal to the plane Γ and passes through the center of the punch. Under the action of the force P, the punch is pressed into the surface z = 0 of the half-space. Friction forces between the punch and the half-space are neglected.

Under the action of a centrally applied force P, the punch penetrates at the depth δ in the direction of the z axis, χ is the contact depth (see Fig. 4), 2α is the apex angle of the cone, then $\cot\alpha = \chi/a$.

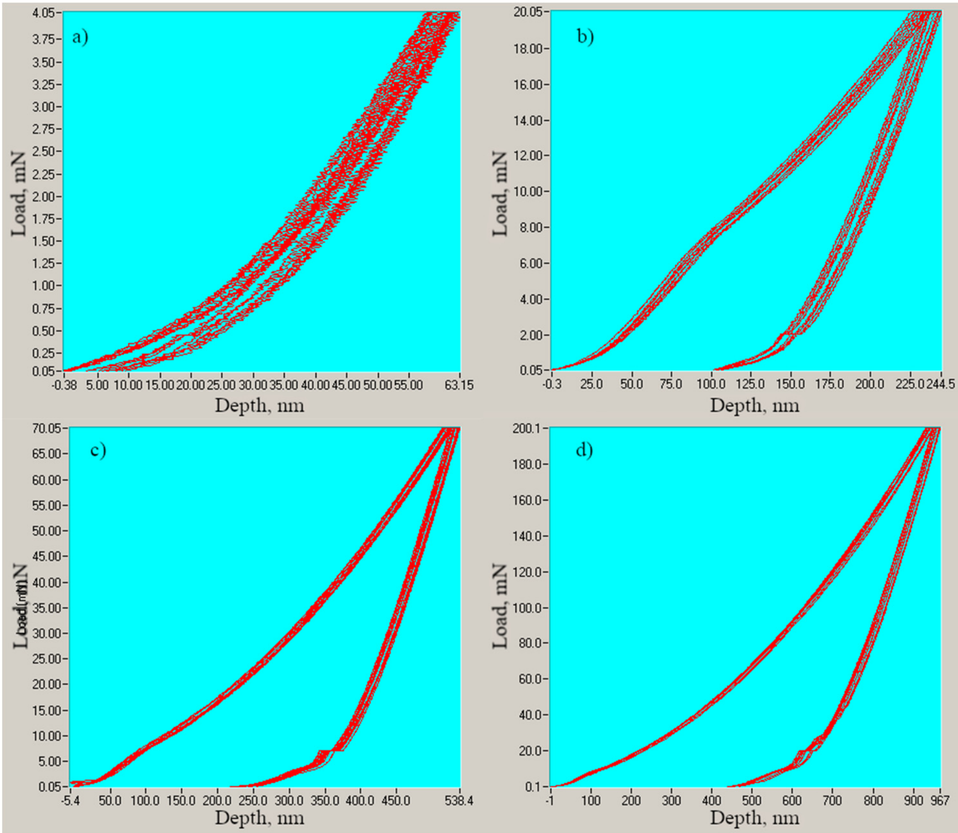

Figure 3: Force–displacement curves obtained by indentation of a three-layer package with a force P_{max}. (a) 4 mN; (b) 20 mN; (c) 70 mN; and (d) 200 mN.

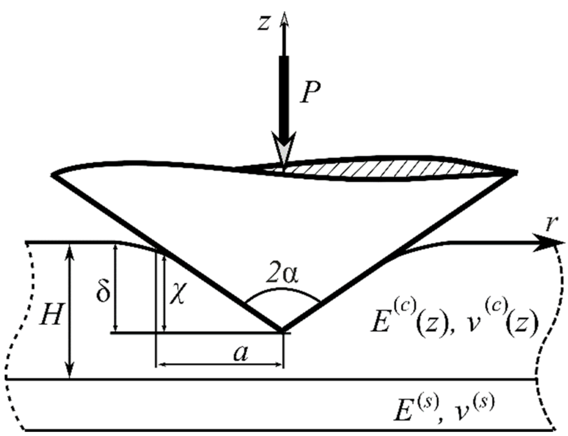

Figure 4: Statement of the problem of indentation of a conical punch into an inhomogeneous half-space.

Young's modulus and Poisson's ratio of the coating and substrate may vary with depth. In the general case, one can assume

$$E(z)=\begin{cases}E_{(c)}(z) & -H\le z\le 0\\ E_{(s)} & -\infty<z<-H\end{cases},\quad \upsilon(z)=\begin{cases}\upsilon^{(c)}(z), & -H\le z\le 0\\ \upsilon^{(s)}, & -\infty<z<-H.\end{cases} \tag{1}$$

We will assume that on the boundary between the coating (superscript (1)) and the substrate (superscript (2)) the following condition is satisfied:

$$z=-H:\quad \begin{cases}\tau_{zr}^1=\tau_{zr}^2,\ \sigma_z^1=\sigma_z^2\\ w^1=w^2,\ u^1=u^2.\end{cases} \tag{2}$$

Outside the contact area, the plane Γ is not loaded. The boundary conditions under the assumptions made are represented as follows:

$$z=0:\ \tau_{zr}^1=\tau_{z\phi}^1=0,\ \begin{cases}\sigma_z^1=0, & \rho>a\\ w^1=-f_a(\rho)=-\left(\delta-\frac{\rho\chi}{a}\right), & \rho\le a.\end{cases} \tag{3}$$

We assume that if $r\to\infty$ and $z\to\infty$ the stresses in the half-space disappear. It is required to determine the relationship between the indentation force and the punch displacement and the law of distribution of normal contact stresses under the punch:

$$\sigma_z|z=0=-\tau_a(\rho),\ \rho\le a. \tag{4}$$

We also assume that the condition of smoothness of contact stresses is satisfied at the edge of the contact area:

$$\tau_a(\rho)=0. \tag{5}$$

By applying the Hankel integral transform, the problem is reduced to solving the following dual integral equation [39]:

$$\begin{cases}\int_0^\infty T(\gamma)L(\lambda\gamma)J_0(r\gamma)d\gamma=\frac{E_{ef}^{(c)}}{2}\frac{(\delta-r\chi)}{a}, & r\le 1\\ \int_0^\infty T(\gamma)J_0(r\gamma)\gamma d\gamma=0, & r>1,\end{cases} \tag{6}$$

where $L(u)$ = kernel transform of the integral equation, $J_0(u)$ = Bessel function of the first kind, $r=\rho/a$, $E_{ef}^{(c)}=E^{(c)}(1-(\upsilon^{(c)})^2)^{-1}$, $\tau(r)=\tau_a(ar)$, $\lambda=H/a$ is the dimensionless coating thickness.

We approximate the kernel transform by the following formula:

$$L(u)\approx L_N(u)=\prod_{i=1}^N\frac{u^2+A_i^2}{u^2+B_i^2},\quad A_i,\ B_i\in C. \tag{7}$$

The solution to this problem is described in detail in Aizikovich et al. [40].

Using the approach described the approximate analytical expressions for the significant mechanical characteristics (stiffness, force, and indentation depth) were obtained:

$$S=2aE_{ef}^{(s)}\frac{P_0(\lambda)}{\delta_0(\lambda)},\quad P=\frac{E_{ef}^{(s)}a\chi}{2}P_0(\lambda),\quad \delta=\frac{\pi\chi}{2}\delta_0(\lambda),\quad \chi=a\,\mathrm{ctg}\,\alpha\ , \tag{8}$$

$$P_0(\lambda)=1+2\lambda\sum_{i=1}^N\left(\frac{C_i}{A_i}\left[\mathrm{ch}(\frac{A_i}{\lambda})-\frac{\lambda}{A_i}\mathrm{sh}(\frac{A_i}{\lambda})\right]+\frac{D_i}{A_i}\left[\frac{\lambda}{A_i}-\frac{\lambda}{A_i}\mathrm{ch}(\frac{A_i}{\lambda})+\mathrm{sh}(\frac{A_i}{\lambda})\right]\right), \tag{9}$$

$$\delta_0(\lambda) = 1 + \sum_{i=1}^{N} \lambda A_i^{-1} \left(C_i \operatorname{ch}(A_i \lambda_{-1}) + D_i \operatorname{sh}(A_i \lambda_{-1}) \right). \tag{10}$$

where S is indentation stiffness, $E_{ef}^{(s)} = E^{(s)}(1-(\upsilon^{(s)})^2)^{-1}$ is the effective elastic modulus of the substrate (GPa); A_i, C_i, D_i are dimensionless constants that depend on the elastic properties of the coating and substrate [41]. Eqns (10)–(12) are asymptotically exact as $\lambda \to 0$ and $\lambda \to \infty$. The functions $P_0(\lambda)$ and $\delta_0(\lambda)$ describe the influence of the coating on the characteristics of the contact. If the coating thickness tends to zero ($\lambda \to 0$), then $P_0(\lambda) \to 0$, $\delta_0(\lambda) \to 0$, and therefore eqn (10) coincides with the formulas for a homogeneous half-space without a coating [41]. The apex angle of the cone is chosen similarly to Golovin [4], based on the following considerations. Let A_C^{Berk} be the area of the contact area during application of the Berkovich indenter, obtained from the instrument calibrations: $A_c^{\text{Berk}} = 23.33\chi_2 + 3213.76\chi$, and A_C^{Con} is the area of the contact area during the application of a conical punch. For geometrical reasons $A_c^{\text{con}} = \pi a_2 = \pi\chi \tan_2 \alpha$. Equating $A_c^{\text{Berk}} = A_c^{\text{con}}$ one obtains

$$\alpha = \frac{180}{\pi} \operatorname{arccot}\left(\frac{17{,}725\sqrt{\chi}}{\sqrt{2333\chi + 321300}} \right). \tag{11}$$

Fig. 5 shows the diagram of the averaged values with standard deviations of the effective Young's modulus of the coating, obtained experimentally using nanoindentation.

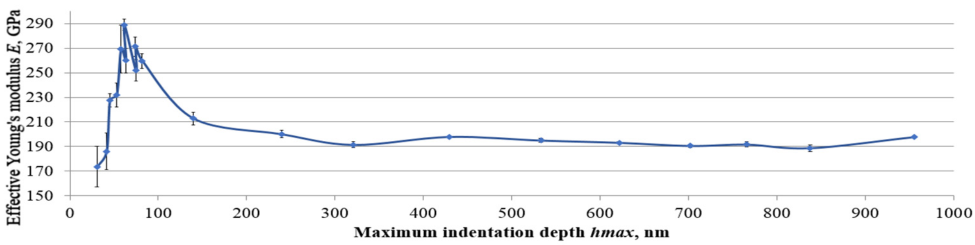

Figure 5: Experimental results of the nanoindentation tests.

The theoretical results for the low indentation forces were obtained by employing the mathematical model. The character of the behaviour of the theoretical and experimental Young's moduli are found to be similar, however the results of the modelling demonstrated a shift along the x-axis in the positive direction thus giving overestimated values. This observation is presumably due to hardening processes in the coating associated with the bending of the loading branch of the force–displacement curves visible at around 75 nm indentation depth. This interesting fact is subject to further analysis especially taking into account the previous results when this model accurately described the experimental results for ZrN coatings on the different substrates [42], [43], two-layered NiO-Ni coating [44] and indentation at elevated temperatures [45]. Another possibility to clarify the mechanical behavior of the coating is employing FEM modelling in the way similar to that applied by Wang et al [46] as well as Cao and Chen [47].

The fact that the experimental values observed at the low loads demonstrate underestimated values can be also explained by the influence of nanogeometry of the coating at small indentation depths [48] and the effects of the substrate [49]. According to the available data [48], the indentation depth should be 20 times greater than the average roughness value. If this condition is not met, the measured modulus may be determined incorrectly due to incomplete contact of the indenter with the sample surface and, as a result, change in the actual contact area and decrease in depth compared to the calculated one. According to our own experience and known results [50], in order to eliminate and minimize these effects, it is necessary that the indentation depth of the indenters be less than 10% of the coating thickness [51]. Thus, the measured properties of the coating can be represented as a combination of two superimposed fields (the influence of the substrate and surface geometry) and the true properties of the coating material can only be experimentally studied under the condition that these fields do not intersect and the contact depth of the indenter lies between these conditional fields. Thus, for a coating with a given value of average roughness, there is a minimum thickness at which it is possible to measure the real elastic properties of the coating material. A detailed study and analysis of a large amount of experimental data is necessary for the future works.

4 CONCLUSIONS

This paper presents an efficient mathematical model for describing experiments on the indentation of a sample, namely a ZnO coating obtained by pulsed laser deposition on a silicon substrate. Elemental analysis of the coating has shown good deposition quality and confirmed the good stoichiometric composition of the layer. Using SEM and AFM, the microgeometrical characteristics of the coating surface were studied, which made it possible to select the parameters for nanoindentation. Based on the Oliver–Pharr method, the Young's modulus of the substrate and the effective Young's modulus of the coating-substrate system were determined. To study the Young's modulus of the coating, a series of experiments on nanoindentation has been carried out, followed by mathematical modelling of this process with high (up to tenths of a percent) accuracy. The theoretical and experimental results are in good agreement, however, a slight increase in the theoretical values of Young's modulus has been found in the form of a shift in the theoretical diagram.

ACKNOWLEDGEMENTS

The study was carried out at the Research and Education Center "Materials" of the Don State Technical University (https://nano.donstu.ru/) and supported by the grant of the Government of the Russian Federation No. 14.Z50.31.0046.

REFERENCES

[1] Grodzinski, P.P., 'Elastic' and 'Plastic' hardness of hard materials. *Nature*, **169**(4309), pp. 925–926, 1952.
[2] Ternovsky, A.P. et al., On micromechanical testing of materials by indentation. *Zavod. Lab*, **39**(10), pp. 1242–1246, 1973.
[3] Bulychev, S.I., Alekhin, V.P., Shorshorov, M.Kh., Ternovsky, A.P. & Shnyrev, G.D., Determination of the Young's modulus from the indentation diagram. *Zavod. Lab.*, **41**(9), pp. 1137–1141, 1975.
[4] Golovin, Y.I., Nanoindentation and mechanical properties of solids in submicrovolumes, thin near-surface layers, and films: A Review. *Physics of the Solid State*, **50**(12), pp. 2205–2236, 2008.
[5] Fischer-Cripps, A.C. & Nicholson, D.W., Nanoindentation. *Appl. Mech. Rev.*, **57**(2), pp. B12–B12, 2004.
[6] Oliver, W.C. & Pharr, G.M., An improved technique for determining hardness and elastic modulus using load and displacement sensing indentation experiments. *Journal of Materials Research*, **7**(6), pp. 1564–1583, 1992.

[7] Doerner, M.F. & Nix, W.D., A method for interpreting the data from depth-sensing indentation instruments. *Journal of Materials Research*, **1**(4), pp. 601–609, 1986.

[8] Sadyrin, E.V., Mitrin, B.I., Aizikovich, S.M. & Zubar, T.I., Effect of temperature on the mechanical properties of multi-component Al-Mg-Si alloys during nanoindentation test. *Mater. Phys. Mech.*, **28**, pp. 6–10, 2016.

[9] Sadyrin, E., Swain, M., Mitrin, B., Rzhepakovsky, I., Nikolaev, A., Irkha, V., Yogina, D., Lyanguzov, N., Maksyukov, S. & Aizikovich, S., Characterization of enamel and dentine about a white spot lesion: Mechanical properties, mineral density, microstructure and molecular composition. *Nanomaterials*, **10**(9), p. 1889, 2020.

[10] Sadyrin, E.V., Kislyakov, E.A., Karotkiyan, R.V., Yogina, D.V., Drogan, E.G., Swain, M.V., Maksyukov, S.Yu., Nikolaev, A.L. & Aizikovich, S.M., Influence of citric acid concentration and etching time on enamel surface roughness of prepared human tooth: In vitro study. *Plasticity, Damage and Fracture in Advanced Materials*, Springer: Cham, pp. 135–150, 2020.

[11] Mahoney, E., Holt, A., Swain, M. & Kilpatrick, N., The hardness and modulus of elasticity of primary molar teeth: an ultra-micro-indentation study. *Journal of Dentistry*, **28**(8), pp. 589–594, 2000.

[12] Mahoney, E.K., Rohanizadeh, R., Ismail, F.S.M., Kilpatrick, N.M. & Swain, M.V., Mechanical properties and microstructure of hypomineralised enamel of permanent teeth. *Biomaterials*, **25**(20), pp. 5091–5100, 2004.

[13] Kuprin, A.S., Gilewicz, A., Kuznetsova, T.A., Lapitskaya, V.A., Tolmachova, G.N., Warcholinski, B., Aizikovich, S. & Sadyrin, E.V., Structure and properties of ZrON coatings synthesized by cathodic arc evaporation. *Materials*, **14**(6), p. 1483, 2021.

[14] Melnikova, G., Kuznetsova, T., Lapitskaya, V., Petrovskaya, A., Chizhik, S., Zykova, A., Safonov, V., Aizikovich, S., Sadyrin, E., Sun, W. & Yakovin, S., Nanomechanical and nanotribological properties of nanostructured coatings of tantalum and its compounds on steel substrates. *Nanomaterials*, **11**(9), p. 2407, 2021.

[15] Gilewicz, A., Kuznetsova, T., Aizikovich, S., Lapitskaya, V., Khabarava, A., Nikolaev, A. & Warcholinski, B., Comparative investigations of AlCrN coatings formed by cathodic arc evaporation under different nitrogen pressure or arc current. *Materials*, **14**(2), p. 304, 2021.

[16] Vasiliev, A.S., Volkov, S.S., Belov, A.A., Litvinchuk, S.Y. & Aizikovich, S.M., Indentation of a hard transversely isotropic functionally graded coating by a conical indenter. *International Journal of Engineering Science*, **112**, pp. 63–75, 2017.

[17] Vasiliev, A.S., Volkov, S.S., Sadyrin, E.V. & Aizikovich, S.M., Simplified analytical solution of the contact problem on indentation of a coated half-space by a conical punch. *Mathematics*, **8**(6), p. 983, 2020.

[18] Dhong, C. et al., Role of indentation depth and contact area on human perception of softness for haptic interfaces. *Science Advances*, **5**(8), eaaw8845, 2019.

[19] Kot, M., Rakowski, W., Lackner, J.M. & Major, L., Analysis of spherical indentations of coating-substrate systems: Experiments and finite element modeling. *Materials and Design*, **43**, pp. 99–111, 2013.

[20] Karimpour, M., Balint, D.S., Rzepiejewska-Malyska, K.A., Szerling, A., Michler, J. & Lin, J., An inverse method for extracting the mechanical properties of the constituent materials of a multilayer from nanoindentation data. *Computational Materials Science*, **68**, pp. 384–390, 2013.

[21] Dean, J., Aldrich-Smith, G. & Clyne, T.W., Use of nanoindentation to measure residual stresses in surface layers. *Acta Materialia*, **7**(59), pp. 2749–2761, 2011.

[22] Veprek-Heijman, M.G.J. & Veprek, S., The deformation of the substrate during indentation into superhard coatings: Bückle's rule revised. *Surface and Coatings Technology*, **284**, pp. 206–214, 2015.

[23] Wang, C., Luo, S., Liu, C., Liu, X. & Chen, C., Photocatalytic performance of single crystal ZnO nanorods and ZnO nanorods films under natural sunlight. *Inorganic Chemistry Communications*, **114**, 107842, 2020.

[24] Mueen, R., Morlando, A., Qutaish, H., Lerch, M., Cheng, Z. & Konstantinov, K., ZnO/CeO2 nanocomposite with low photocatalytic activity as efficient UV filters. *Journal of Materials Science*, **55**(16), pp. 6834–6847, 2020.

[25] Alhammadi, S., Park, H. & Kim, W.K., Optimization of intrinsic ZnO thickness in Cu (In, Ga) Se2-based thin film solar cells. *Materials*, **12**(9), p. 1365, 2019.

[26] Saboor, A., Shah, S.M. & Hussain, H., Band gap tuning and applications of ZnO nanorods in hybrid solar cell: Ag-doped verses Nd-doped ZnO nanorods. *Materials Science in Semiconductor Processing*, **93**, pp. 215–225, 2019.

[27] Yun, S., Guo, T., Li, Y., Gao, X., Huang, A. & Kang, L., Well-ordered vertically aligned ZnO nanorods arrays for high-performance perovskite solar cells. *Materials Research Bulletin*, **130**, 110935, 2020.

[28] Hunge, Y.M., Yadav, A.A., Kulkarni, S.B. & Mathe, V.L., A multifunctional ZnO thin film based devices for photoelectrocatalytic degradation of terephthalic acid and CO_2 gas sensing applications. *Sensors and Actuators B: Chemical*, **274**, pp. 1–9, 2018.

[29] Shetti, N.P., Bukkitgar, S.D., Reddy, K.R., Reddy, C.V. & Aminabhavi, T.M., ZnO-based nanostructured electrodes for electrochemical sensors and biosensors in biomedical applications. *Biosensors and Bioelectronics*, **141**, 111417, 2019.

[30] Devi, K.R., Selvan, G., Karunakaran, M., Kasirajan, K., Chandrasekar, L.B., Shkir, M. & AlFaify, S., SILAR-coated Mg-doped ZnO thin films for ammonia vapor sensing applications. *Journal of Materials Science: Materials in Electronics*, **31**(13), pp. 10186–10195, 2020.

[31] Shetti, N.P., Bukkitgar, S.D., Reddy, K.R., Reddy, C.V. & Aminabhavi, T.M., ZnO-based nanostructured electrodes for electrochemical sensors and biosensors in biomedical applications. *Biosensors and Bioelectronics*, **141**, 111417, 2019.

[32] Nikolaev, A.L., Kamencev, A.S., Lyanguzov, N.V. & Aizikovich, S.M., Pulsed laser deposition of Au nanoparticles on ZnO nanostructures. *Materials Science and Engineering*, **1029**(1), 012064, 2021.

[33] Pushkariov, V.I., Nikolaev, A.L. & Kaidashev, E.M., Synthesis and characterization of ZnO nanorods obtained by catalyst-free thermal technique. *Journal of Physics*, **541**(1), 012031, 2014.

[34] Khalid, N.R., Hammad, A., Tahir, M.B., Rafique, M., Iqbal, T., Nabi, G. & Hussain, M.K., Enhanced photocatalytic activity of Al and Fe co-doped ZnO nanorods for methylene blue degradation. *Ceramics International*, **45**(17), pp. 21430–21435, 2019.

[35] Mahardika, T., Putri, N.A., Putri, A.E., Fauzia, V., Roza, L., Sugihartono, I. & Herbani, Y., Rapid and low temperature synthesis of Ag nanoparticles on the ZnO nanorods for photocatalytic activity improvement. *Results in Physics*, **13**, 102209, 2019.

[36] Zhilin, D.A., Lyanguzov, N.V., Nikolaev, L.A., Pushkariov, V.I. & Kaidashev, E.M., Photoelectric properties of MSM structure based on ZnO nanorods, received by thermal evaporation and carbothermal syntesis. *Journal of Physics*, **541**(1), 012038, 2014.

[37] Gan, L., Ben-Nissan, B. & Ben-David, A., Modeling and finite element analysis of ultra-microhardness indentation of thin films. *Thin Solid Films*, **290**, pp. 362–366, 1996.
[38] Yang, P.F., Wen, H.C., Jian, S.R., Lai, Y.S., Wu, S. & Chen, R.S., Characteristics of ZnO thin films prepared by radio frequency magnetron sputtering. *Microelectronics Reliability*, **48**(3), pp. 389–394, 2008.
[39] Vasiliev, A.S., Swain, M.V., Aizikovich, S.M. & Sadyrin, E.V., Torsion of a circular punch attached to an elastic half-space with a coating with periodically depth-varying elastic properties. *Archive of Applied Mechanics*, **86**(7), pp. 1247–1254, 2016.
[40] Aizikovich, S.M., Vasil'ev, A.S. & Volkov, S.S., The axisymmetric contact problem of the indentation of a conical punch into a half-space with a coating inhomogeneous in depth. *Journal of Applied Mathematics and Mechanics*, **79**(5), pp. 500–505, 2015.
[41] Sneddon, I.N., *Fourier Transforms*, McGraw-Hill: New York, 542 pp., 1951.
[42] Vasiliev, A.S., Sadyrin, E.V., Mitrin, B.I., Aizikovich, S.M. & Nikolaev, A.L., Nanoindentation of ZrN coatings on silicon and copper substrates. *Russian Engineering Research*, **38**(9), pp. 735–737, 2018.
[43] Sadyrin, E., Vasiliev, A. & Volkov, S., Mathematical modeling of experiment on Berkovich nanoindentation of ZrN coating on steel substrate. *Acta Polytechnica CTU Proceedings*, **27**, pp. 18–21, 2020.
[44] Sadyrin, E.V., Mitrin, B.I., Krenev, L.I., Nikolaev, A.L. & Aizikovich, S.M., Evaluation of mechanical properties of the two-layer coating using nanoindentation and mathematical modeling. *International Conference on Physics and Mechanics of New Materials and Their Applications*, Springer: Cham, pp. 495–502, 2017.
[45] Krenev, L.I., Volkov, S.S., Sadyrin, E.V., Zubar, T.I. & Chizhik, S.A., Mechanical material tests by the nanoindentation method at various indenter and specimen temperatures. *Journal of Engineering Physics and Thermophysics*, **91**(3), pp. 594–600, 2018.
[46] Wang, J.S., Zheng, X.J., Zheng, H., Song, S.T. & Zhu, Z., Identification of elastic parameters of transversely isotropic thin films by combining nanoindentation and FEM analysis. *Computational Materials Science*, **49**(2), pp. 378–385, 2010.
[47] Cao, G. & Chen, X., The size effect of nanoindentation on ZnO nanofilms. *Journal of Applied Physics*, **102**(12), 123513, 2007.
[48] ISO 14577-1:2002 Metallic materials – Instrumented indentation test for hardness and materials parameters – Part 1: Test method.
[49] Gamonpilas, C. & Busso, E.P., On the effect of substrate properties on the indentation behaviour of coated systems. *Materials Science and Engineering: A*, **380**(1–2), pp. 52–61, 2004.
[50] Sun, Y., Bell, T. & Zheng, S., Finite element analysis of the critical ratio of coating thickness to indentation depth for coating property measurements by nanoindentation. *Thin Solid Films*, **258**(1–2), pp. 198–204, 1995.
[51] He, J.L. & Veprek, S., Finite element modeling of indentation into superhard coatings. *Surface and Coatings Technology*, **163**, pp. 374–379, 2003.